NONLINEAR DYNAMIC MODELING OF MICROMACHINED MICROWAVE SWITCHES*

E.K. Chan, E.C. Kan and R.W. Dutton
Center for Integrated Systems
P. M. Pinsky
Department of Mechanical Engineering
Stanford University, Stanford, CA 94305

ABSTRACT

Nonlinear dynamic lumped models of micromachined microwave switches have been formulated and successfully applied to analyses of transient characteristics and geometrical scaling. Parameter extraction through electrical measurements is summarized. The results are compared to transient quasi-2D simulations.

I. INTRODUCTION

The electrostatically-actuated micromachined switch [1], which is shown in cross-section in Fig.1,

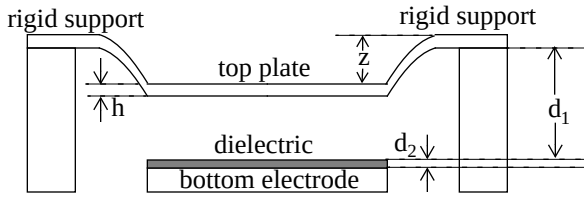

Fig. 1: Cross-section of micromachined switch

has great potential for microwave applications due to its extremely low intermodulation distortion and integrated circuit backend technology compatibility. Figs. 2 and 3 show two different plan views of the switch. The Type I switch consists of a center

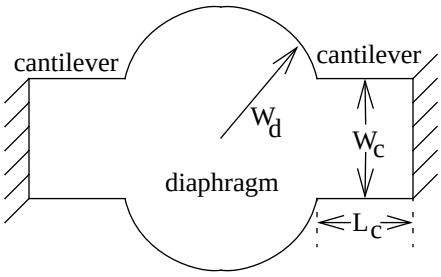

Fig. 2: Plan view of Type I switch

diaphragm supported by two cantilevers whereas the Type II switch has a center diaphragm narrower than the edge supports. In the past, the switch has been modeled as a parallel plate capacitor and a linear spring

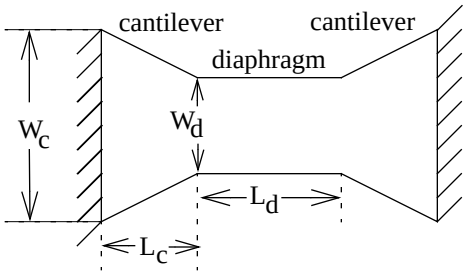

Fig. 3: Plan view of Type II switch

at static equilibrium [2] as shown in Fig. 4. 3D finite element simulations have been used to examine more detailed geometrical effects [3] but are computationally expensive and mostly limited to static analyses. We have formulated nonlinear dynamic lumped models which capture the effects of electrostatics, bending, stretching, residual stress, inertia, squeeze film damping, Van der Waals forces, and contact. These models allow the designer to perform efficient transient analyses, lumped parameter extraction, and

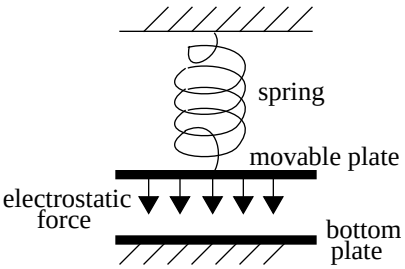

Fig. 4: Spring-capacitor model

geometrical scaling studies. We compare the results with quasi-2D analyses of the micromachined switch.

II. NON-LINEAR DYNAMIC ONE-LUMP MODEL

The Type I switch can be modeled as a rigid diaphragm supported by two cantilevers resulting in a single nonlinear spring-mass system. The geometrical parameters are illustrated in Figs. 1, 2 and 3. The equation of motion of the diaphragm is

$$F_{bend} + F_{stretch} + F_{stress} + F_{electro} \qquad (1)$$

$$+ F_{damp} + F_{VDW} + F_{contact} = m\frac{d^2 z}{dt^2}$$

. *This work was supported by DARPA contract # F30602-96-2-0308- P00001.

where m is the mass of the diaphragm and the cantilever, and z is the displacement of the diaphragm. The linear bending force of an end-loaded cantilever, accurate up to rotations of 0.2 radians, is given by [4]

$$F_{bend} = -\frac{2 \times 3 \times EI}{L_c^3} z \qquad (2)$$

where E is the plate modulus of elasticity, and I is the moment of inertia of the cantilever. The nonlinear force due to the stretching of the deflecting cantilever is

$$F_{stretch} = -\frac{2 \times 16 h W_c E (1-\upsilon)}{9 L_c^3} z^3 \qquad (3)$$

where υ is Poisson's ratio. Residual stress, σ, adds a stiffness force given by

$$F_{stress} = -\frac{2 \times 4 h W_c \sigma}{3 L_c} z. \qquad (4)$$

The electrostatic attraction set up by an applied voltage, V, is described by

$$F_{electro} = \frac{\varepsilon A V^2}{2\left(d_1 + \frac{d_2}{\kappa} - z\right)^2} \qquad (5)$$

where ε is the permittivity of free space, κ is the relative dielectric constant of the thin dielectric above the bottom plate, and A is the area of the diaphragm. Squeeze-film damping is approximated as [5]

$$F_{damp} = -\frac{\mu A W_d^{\,2}}{d_1^{\,3}} \frac{dz}{dt} \qquad (6)$$

where μ is the viscosity. When the diaphragm comes into contact with the bottom dielectric layer, Van der Waals and repulsive forces, as shown below, become important [6]:

$$F_{VDW} + F_{contact} = \frac{K_1 A}{(d_1 - z)^3} - \frac{K_2 A}{(d_1 - z)^{10}} \qquad (7)$$

K_1 determines the surface energy due to the Van der Waals attraction whereas K_2 determines the equilibrium distance from the surface. These numbers depend very strongly on the microstructure of the surface.

The one lump model can model the Type I switch quite accurately since most of the deformation occurs in the narrower cantilever supports rather than in the diaphragm.

III. Non-Linear Dynamic Two-Lump Model

In the Type II switch, significant deformation occurs in both the diaphragm and cantilever supports. This switch can be modeled as cantilevers supporting a flexible beam through pin joints as shown in Fig. 5. The equation of motion of the two-spring-two-mass system is

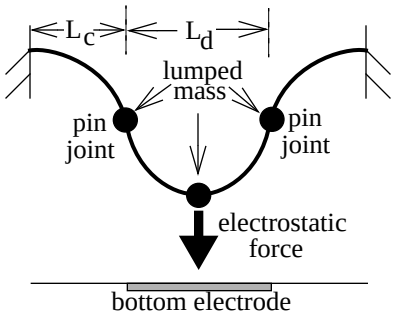

Fig. 5: Cantilever + Pin joint + Flexible beam

$$F^c_{bend} + F^c_{stretch} + F^c_{stress} + F^c_{damp} + F^c_{VDW} + F^c_{contact} - F^d_{bend} - F^d_{stretch} - F^d_{stress} = m_c \frac{d^2 z_c}{dt^2} \qquad (8)$$

$$F^d_{bend} + F^d_{stretch} + F^d_{stress} + F^d_{electro} + F^d_{damp} + F^d_{VDW} + F^d_{contact} = m_d \frac{d^2 z_d}{dt^2} \qquad (9)$$

where the superscripts and subscripts c and d denote cantilever and diaphragm respectively. The forces on the cantilever were described in Section I. However, the effective area of the Van der Waals and contact forces is very small since only the tip of the cantilever can touch the bottom dielectric. The forces on the diaphragm, which is modeled as a center-loaded simply-supported beam are [4]:

$$F^d_{bend} = -\frac{48 \times EI_d}{L_d^3}(z_d - z_c) \qquad (10)$$

$$F^d_{stretch} = -\frac{\pi^4 h W_d E (1-\upsilon)}{4 L_d^3}(z_d - z_c)^3 \qquad (11)$$

$$F^d_{stress} = -\frac{\pi^2 h W_d \sigma (1-\upsilon)}{2 L_d}(z_d - z_c) \qquad (12)$$

IV. Quasi-2D Simulation

Instead of describing the deflection of the switch with just one or two lumps, we can consider the cantilever and diaphragm together as a flexible beam with fixed end supports and discretize it into a number of segments, each of which obeys the equation of motion, Eq. 1. In the distributed case, the mechanical forces (per unit length) on each segment are given by [7]

$$F_{bend} = -\frac{\partial^2}{\partial x}\left(EI\frac{\partial^2 z}{\partial x^2}\right) \quad (13)$$

$$F_{stress} = -hW(1-\upsilon)\sigma\frac{\partial^2 z}{\partial x^2} \quad (14)$$

$$F_{stretch} = -hWE(1-\upsilon)\left[\frac{1}{L_{tot}}\int_o^{L_{tot}}\frac{1}{2}\left(\frac{\partial z}{\partial x}\right)^2 dx\right]\frac{\partial^2 z}{\partial x^2} \quad (15)$$

where x is the horizontal coordinate, W is the width of each discrete segment, and $L_{tot} = L_d + 2L_c$. The electrostatic, damping, Van der Waals and contact forces are all similar in form to Eqs. 5-7, substituting width for area, A, since the forces in Eqs. 8 and 9 are per unit length. This quasi-2D model assumes that all forces, and hence all motion, are vertical.

The quasi-2D model allows us to model stiction effects by examining how the Van der Waals force causes the diaphragm to peel off the bottom dielectric rather than lift off as a whole when the switch is turned off.

We can refine the one-lump and two-lump models by fitting the force-displacement relationships in Eqs. 2-4 and 10-12 -- nominally either linear or cubic -- to actual force-displacement characteristics extracted from quasi-2D simulations. The effective length of the cantilever in the two-lump model -- the length from the fixed end to the point where the curvature of the deformed structure changes sign -- can be extracted from quasi-2D simulations also. For large-scale simulation in a VLSI circuit with an array of switches, the lumped models are more efficient computationally.

V. Simulation Results

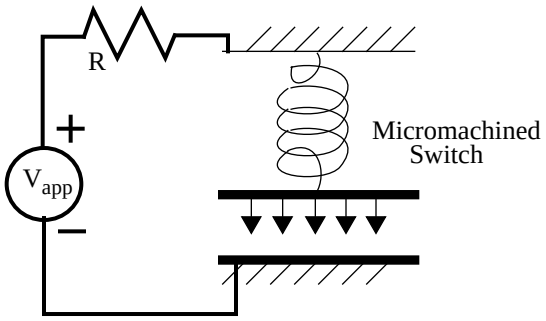

Fig. 6: Actuating circuit for parameter extraction

Fig. 6 shows the micromachined switch embedded in an actuating circuit. Switching threshold voltages are plotted as a function of diaphragm radii for Type I switches in Fig. 7. This compares well with measured data shown in [1]. Fig. 8 shows the transient on-off response of a Type I micromachined switch simulated using the one-lump model, and a Type II switch using the two-lump model. Since it is relatively easy to control the resistance and applied voltage, parameter extraction can be accomplished by a least-squares fitting of the simulated transient characteristics to actual measurements with varying R and V_{app}. Fig. 9 shows the turn-on time, t_{on}, as a function of applied voltage for different values of viscosity. Fig. 10 shows t_{on} to be a weak function of plate modulus, E. The

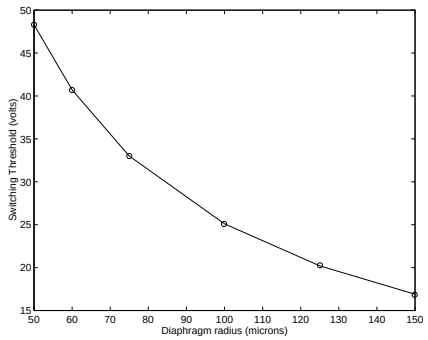

Fig. 7: Variation of switching threshold as a function of diaphragm radius for Type I switches (other parameters held constant)

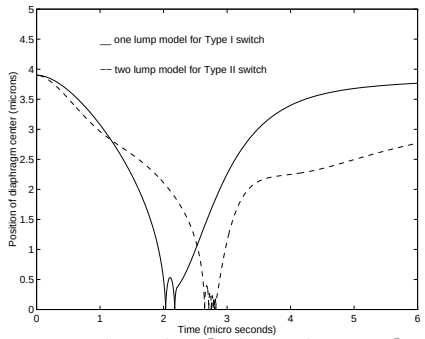

Fig. 8: Transient simulation using one lump and two lump models

circuit resistance also has the beneficial effect of damping out oscillations when the diaphragm hits the thin dielectric thus allowing the switch to settle quickly. This resistance has negligible impact on turn-on characteristics, but should be removed from the circuit when the switch is to be turned off.

After material parameters have been determined, the model can be used for scaling studies to optimize the geometry of the device. Figs. 11 through 13 show how t_{on} and t_{off} change as functions of geometrical parameters such as cantilever length, thickness, and diaphragm size. The trade-offs between t_{on} and t_{off} are evident.

The accuracy of the lumped models can be

enhanced by including form factors which can account for fringing fields, and distributed rather than concentrated loads and masses.

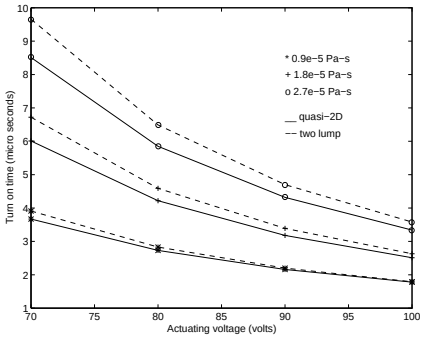

Fig. 9: t_{on} vs actuating voltage for various μ

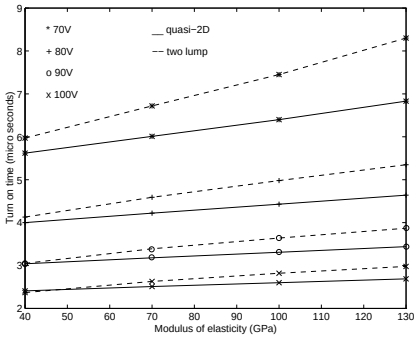

Fig. 10: Variation of t_{on} with E for various V_{app}

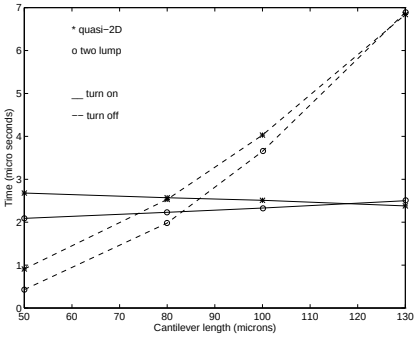

Fig. 11: Variation of t_{on} and t_{off} with cantilever length in Type II switch

VI. CONCLUSION

These nonlinear dynamic lumped models of micromachined switches can be used by a designer for efficient transient analyses, parameter extraction and geometrical scaling studies. All important physical phenomena have been taken into account.

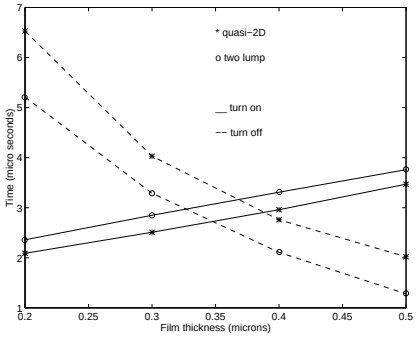

Fig. 12: Variation of t_{on} and t_{off} with film thickness, h, in Type II switch

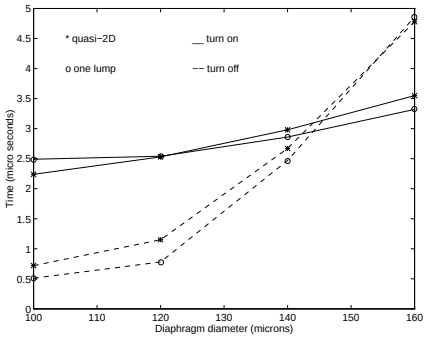

Fig. 13: Variation of t_{on} and t_{off} with diaphragm diameter, W_d, in Type I switch

REFERENCES

[1] C. Goldsmith, J. Randall, S. Eshelman, T.H. Lin, "Characteristics of micromachined switches at microwave frequencies," *MTT-S 1996 Technical Digest*, pp 1141-1144.

[2] H.C. Nathanson, W.E. Newell, R.A. Wickstrom, J.R. Davis, "The resonant gate transistor," *IEEE Transactions on Electron Devices*, Vol ED-14, No. 3, March 1967, pp 117-133.

[3] B.E. Artz, L.W. Cathey, "A finite element method for determining structural displacements resulting from electrostatic forces," *Tech Digest IEEE Solid State Sensor and Actuator Workshop,* Hilton Head Island, June 1992, pp 190-193.

[4] R.J. Roark, W.C. Young, *Formulas for Stress and Strain*, McGraw-Hill, New York, 1975.

[5] J.B. Starr, "Squeeze-film damping in solid-state accelerometers," *Tech Digest IEEE Solid State Sensor and Actuator Workshop*, Hilton Head Island, June 1990, pp 44-47.

[6] C. Kittel, *Introduction to Solid State Physics*, John Wiley & Sons Inc, 1996.

[7] S.P. Timoshenko, J.M. Gere, *Mechanics of Materials*, D. Van Nostrand Co., 1972.